

THE SATURATED REGIME OF A SEEDED SINGLE-PASS FREE ELECTRON LASER: A THEORETICAL INVESTIGATION THROUGH THE STATISTICAL MECHANICS OF THE VLASOV EQUATION

F. Curbis*, University of Trieste & Elettra, Basovizza, Trieste, Italy,
 A. Antoniazzi, Dipartimento di Energetica, Università di Firenze, Italy
 G. De Ninno, Elettra, Basovizza, Trieste, Italy,
 D. Fanelli, Dipartimento di Energetica, Università di Firenze, Italy.

Abstract

The quasi-stationary state characterizing the saturation of a single-pass free-electron laser is governed by the Vlasov equation obtained by performing the continuum limit of the Colson-Bonifacio model. By means of a statistical treatment, this approach allows to predict analytically the saturated laser intensity as well as the final electron-beam energy distribution. In this paper we consider the case of coherent harmonic generation obtained from a seeded free-electron laser and present predictions for the first stage of the project FERMI@Elettra project at Sincrotrone Trieste.

INTRODUCTION

In a single-pass FEL, the physical mechanism responsible for the light emission and amplification is the interaction between a relativistic electron beam, a magnetostatic periodic field generated by an undulator and an optical wave co-propagating with electrons. Two different schemes can be distinguished, depending on the origin of the optical wave which is used to initiate the process. In the SASE configuration, the initial seed is provided by the spontaneous emission of the electron beam which is forced by the undulator field to follow a curved trajectory. The seed is then amplified all along the undulator until the laser effect is reached. The SASE radiation produces tunable signal at short (x-ray) wavelengths with several GW peak power and excellent spatial mode. An alternate approach to SASE is Coherent Harmonic Generation (CHG) [1], which is capable of producing temporally coherent pulses. A schematic layout of CHG is shown in Figure 1.

In this case, the initial seed is produced by an external light source, e.g. a laser. The light-electron interaction in a short undulator, called modulator, imposes an energy modulation on the electron beam. The modulator is tuned to the seed wavelength λ . The energy modulation is then converted into a spatial density modulation as the electron beam transverses a magnetic dispersion. Figure 2 shows the evolution of the electron-beam phase space (i.e. energy vs. electrons' phase in the undulator plus radiator field) from the entrance of the modulator to the exit of the dis-

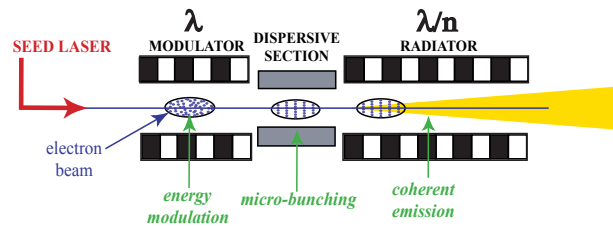


Figure 1: Schematic layout of the CHG scheme.

persive section. Finally, in a second undulator, called radiator and tuned at the n -th harmonic of the seed frequency, the micro-bunched electron beam emits coherent radiation at the harmonic wavelength λ/n . Such a radiation is then amplified until saturation is reached.

Importantly, it shall be noticed that Single-pass FELs represent an example of systems with long-range interactions [2]. When long-range forces are to be considered, a global network of connections between individual constituting elements is active, and *mean-field* effects are dominant. Surprisingly, within the realm of long range interacting systems, a wide number of striking phenomena appear including ensemble inequivalence, negative specific heat and emergence of Quasi-Stationary States (QSS), i.e., long-living states where the system gets eventually trapped before relaxing to its final statistical equilibrium. This latter remarkable non equilibrium feature is also reported for

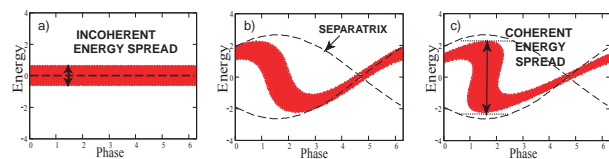


Figure 2: Electron-beam phase space at the entrance a) and at the exit b) of the modulator; c) phase space at the exit of the dispersive section. In a), the thickness of the distribution corresponds to the (initial) incoherent energy spread of the electron beam. In c) the gap between the boundaries of the separatrix corresponds to the energy modulation induced by the seed-electron interaction (see Figure 1).

* francesca.curbis@elettra.trieste.it

FELs, where it plays a central role, being the only state experimentally accessible in real devices. In this respect, FELs provide a general experimental ground to investigate the universal characteristics of systems with long range interactions.

Motivated by this analogy, we shall apply a maximum entropy principle, inspired to Lynden-Bell's theory of "violent relaxation" [3]–[6] for the Vlasov equation and analytically predict the characteristics of the laser signal at saturation. More specifically, the above theoretical interpretative framework will enable us to estimate the expected intensity for the case of FERMI@Elettra [7], a future user-facility based on CHG, without resorting to direct numerical simulations. Our results will be shown to correlate well with Genesis-based [8] estimates.

FROM THE MEAN-FIELD MODEL TO THE LYNDEN-BELL PREDICTION

In this section we will introduce the model that is customarily employed to investigate the time evolution of a single-pass FEL, both in SASE and CHG configurations. By putting forward the hypothesis of one-dimensional (longitudinal) motion and monochromatic radiation, the steady-state dynamics of a single-pass FEL is described by the following set of equations:

$$\frac{d\theta_j}{d\bar{z}} = p_j \quad , \quad (1)$$

$$\frac{dp_j}{d\bar{z}} = -Ae^{i\theta_j} - A^*e^{-i\theta_j} \quad , \quad (2)$$

$$\frac{dA}{d\bar{z}} = i\delta A + \frac{1}{N} \sum_j e^{-i\theta_j} \quad , \quad (3)$$

where $\bar{z} = 2k_u \rho z \gamma_r^2 / \langle \gamma_0 \rangle^2$ is the re-scaled longitudinal coordinate, which plays the role of time. Here, $\rho = (a_w \omega_p / 4ck_u)^{2/3} / \gamma_r$ is the so-called Pierce parameter, γ_r the resonant energy, $\langle \gamma_0 \rangle$ the mean energy of the electrons at the undulator's entrance, k_u the wave vector of the undulator, $\omega_p = (e^2 \bar{n} / m \epsilon_0)^{1/2}$ the plasma frequency, \bar{n} being the electron number density, c the speed of light, e and m respectively the charge and mass of one electron. Further, $a_w = eB_w / (k_u mc^2)$, where B_w is the rms undulator field. Introducing the wavenumber k of the FEL radiation, the phase θ is defined by $\theta = (k + k_u)z - 2\delta \rho k_u z \gamma_r^2 / \langle \gamma_0 \rangle^2$; its conjugate momentum reads $p = (\gamma - \langle \gamma_0 \rangle) / (\rho \langle \gamma_0 \rangle)$. The complex amplitude $A = A_x + iA_y$ represents the scaled field, transversal to z . Finally, the detuning parameter is given by $\delta = (\langle \gamma_0 \rangle^2 - \gamma_r^2) / (2\rho \gamma_r^2)$, and measures the average relative deviation from the resonance condition. The above system of equations (N being the number of electrons) can be deduced by the Hamiltonian:

$$H = \sum_{j=1}^N \frac{p_j^2}{2} - \delta I + 2\sqrt{\frac{I}{N}} \sum_{j=1}^N \sin(\theta_j - \varphi) \quad , \quad (4)$$

where the intensity I and the phase φ of the wave are defined by $A = \sqrt{I/N} \exp(-i\varphi)$. Here, the canonically conjugated variables are (p_j, θ_j) for $1 \leq j \leq N$ and (I, φ) . Besides the "energy" H , the total momentum $P = \sum_j p_j + I$ is also a conserved quantity. Let us finally define the bunching parameter as $b(t) = \sum \exp(i\theta_i(t)) / N := \langle \exp(i\theta(t)) \rangle$. The latter provides a quantitative measure of the degree of spatial compactness of the particles distribution.

Numerical simulations based on the above system of equations show that the amplification of the wave occurs in several subsequent steps. First, an initial exponential growth takes place, which is successfully captured by a linear analysis. Then, as previously anticipated, the system attains a QSS, where the wave intensity displays oscillations around a well-defined plateau. As predicted by the Boltzmann-Gibbs statistics, for longer times a slow evolution toward the final equilibrium is found. The process is driven by granularity and the relaxation time diverges with the system size N . Hence, due to the constraint imposed by the typical length of an undulator, the QSS is the only regime experimentally accessible in the case of single-pass FELs.

When performing the thermodynamics limit, i.e., $N \rightarrow \infty$, one gets to the following Vlasov-wave picture:

$$\frac{\partial f}{\partial \bar{z}} = -p \frac{\partial f}{\partial \theta} + 2(A_x \cos \theta - A_y \sin \theta) \frac{\partial f}{\partial p} \quad , \quad (5)$$

$$\frac{dA_x}{d\bar{z}} = -\delta A_y + \int f \cos \theta d\theta dp \quad , \quad (6)$$

$$\frac{dA_y}{d\bar{z}} = \delta A_x - \int f \sin \theta d\theta dp \quad . \quad (7)$$

which can be shown to govern the initial growth and relaxation towards the QSS. The latter conserves the pseudo-energy per particle

$$h(f, A) = \int \frac{p^2}{2} f(\theta, p) d\theta dp - \delta(A_x^2 + A_y^2) + \int (A_x \sin \theta + A_y \cos \theta) f(\theta, p) d\theta dp \quad (8)$$

and the momentum per particle

$$\sigma(f, A) = \int p f(\theta, p) d\theta dp + (A_x^2 + A_y^2) \quad . \quad (9)$$

In ref. [4] it was shown that the average statistical parameters of the laser (intensity and the bunching in the QSS) are accurately predicted by a statistical mechanics treatment of the Vlasov equation, according to prescriptions of the seminal work by Lynden-Bell [5]. The analysis developed in [4] was limited to the case of spatially homogeneous initial conditions (i.e., initial zero bunching). In [9], we extended the analysis by including initially bunched distributions. In the remaining part of this section we will review the foundation of the analytical method and presented select numerical results.

The basic idea of Lynden–Bell “violent relaxation” theory [4, 6] is to coarse-grain the microscopic single-particle distribution function $f(\theta, p, t)$, which is filamented and stirred by the dynamics. An entropy is then associated to the coarse-grained function \bar{f} , which essentially counts the number of microscopic configurations giving rise to it.

Starting with an initial centered water-bag distribution, which corresponds to a rectangle uniformly occupied in the phase space (θ, p) with $-p_0 < p < p_0$ and $-\theta_0 < \theta < \theta_0$, the normalization condition reads $f_0 = 1/(4\theta_0 p_0)$.

The entropy can be expressed as [5, 6]:

$$s(\bar{f}) = - \int \left[\frac{\bar{f}}{f_0} \ln \frac{\bar{f}}{f_0} + \left(1 - \frac{\bar{f}}{f_0} \right) \ln \left(1 - \frac{\bar{f}}{f_0} \right) \right] d\theta dp. \quad (10)$$

The equilibrium is computed by maximizing this entropy:

$$\max_{\bar{f}, A_x, A_y} (s(\bar{f})), \quad (11)$$

while imposing the dynamical constraints:

$$h(\bar{f}, A_x, A_y) = h_0, \quad (12)$$

$$\sigma(\bar{f}, A_x, A_y) = \sigma_0, \quad (13)$$

$$\int f(\theta, p) d\theta dp = 1, \quad (14)$$

where h_0 and σ_0 stand, respectively, for the energy and momentum (per particle) of the system. Performing the analytical calculation and introducing the rescaled Lagrange multipliers for the energy, momentum and normalization constraints (β/f_0 , λ/f_0 and μ/f_0) one obtains the typical Fermi-Dirac distribution:

$$\bar{f} = f_0 \frac{e^{-\beta(p^2/2 + 2A \sin \theta) - \lambda p - \mu}}{1 + e^{-\beta(p^2/2 + 2A \sin \theta) - \lambda p - \mu}} \quad (15)$$

$$A = \sqrt{A_x^2 + A_y^2} = \frac{\beta}{\beta\delta - \lambda} \int \sin(\theta) \bar{f}(\theta, p) d\theta dp.$$

The three constraints (12)–(14) are then imposed by making use of the above expression for $f(\theta, p)$ and A , and the obtained equations numerically solved to provide an estimate of the multipliers as functions of energy h_0 and momentum σ_0 of the system. Once β , γ , μ are calculated, one can in turn estimate the value of the intensity I and the bunching parameter b of the QSS.

To validate our findings, we performed numerical simulation for a water-bag initial distribution as specified above, where $\theta_0 < \pi$. Further, label with $|b_0|$ the initial bunching, i.e., the positive quantity given by $|b_0| = |\langle \exp(i\theta(0)) \rangle|$. Numerical calculations are performed based on the discrete system (1–3). In Figure 3 the average intensity at saturation is reported as function of $|b_0|$, for different values of the initial kinetic energy. Results are compared with the analytical estimate obtained above. Analogous plots for the average value of the bunching parameter at saturation are

reported in Figure 4. A direct inspection of the figures confirms the adequacy of the proposed theoretical framework: predictions based on the Vlasov theory correlate well with numerical curves. In the next section, starting from these results, we will elaborate a strategy to gain insight into the non-linear evolution of a CGH scheme without resorting to direct numerical investigations. In particular, we will focus on the case of the FERMI@Elettra project.

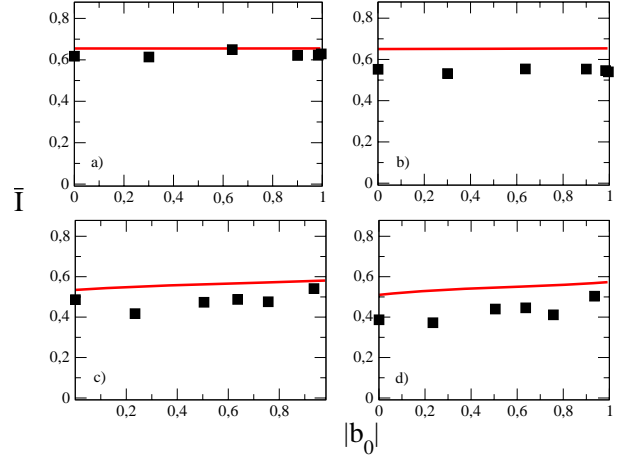


Figure 3: Average intensity \bar{I} at undulator exit as function of the initial bunching $|b_0|$ for different values of the initial average kinetic energy, respectively a) $h_0 = 0.01$ b) $h_0 = 0.16$ c) $h_0 = 0.21$ d) $h_0 = 0.315$. The continuous lines correspond to the Lynden–Bell theoretical prediction, while symbols represent numerical results obtained averaging intensity fluctuations in the saturated regime over ten different realizations of the initial conditions resting on the same values of θ_0 and p_0 .

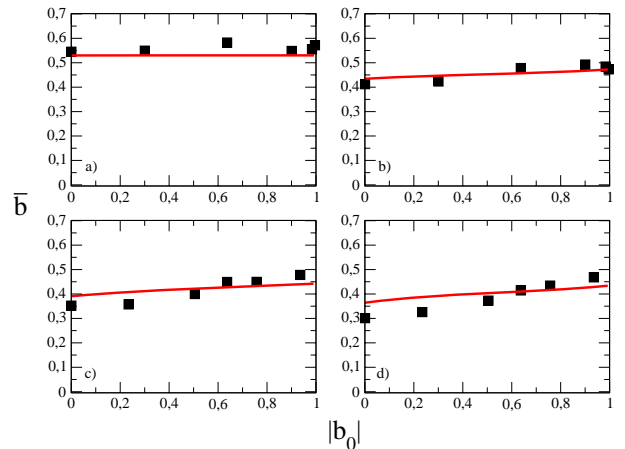


Figure 4: Average values of the bunching parameter \bar{b} at the undulator exit as function of $|b_0|$. Same choice of parameters as in Figure 3.

CHARACTERIZING THE SATURATION OF CHG FELS

The seed-electron interaction in the first undulator of a CHG scheme induces a coherent modulation, $\Delta\gamma$, of the electron-beam energy, which superimposes to the initial incoherent energy spread σ_γ . Inside the dispersive section, the energy modulation is converted into a spatial density modulation. Performing a Fourier analysis of the spatial beam distribution at the end of the dispersive section one finds the following bunching parameters:

$$|b_0| \simeq J_n(n)/\exp(1/2), \quad (16)$$

where J_n stands for the n -th order Bessel function ¹.

On the other hand, the total energy spread $\sigma_{\gamma,tot}$ at the entrance of the second undulator reads:

$$\sigma_{\gamma,tot} = \sqrt{\sigma_\gamma^2 + \frac{(\Delta\gamma)^2}{2}} \simeq \sigma_\gamma \sqrt{1 + \frac{n^2}{2}}, \quad (17)$$

where n is the harmonic number. Moreover, in term of the rescaled variables used in the formulation of the above one-dimensional model, the associated energy profile can be ideally schematized as a water-bag distribution, where

$$p_0 = \frac{\sigma_{\gamma,tot}}{\gamma\rho}. \quad (18)$$

Taking full advantage of the above theoretical analysis, we are therefore in a position to quantify the saturated (QSS) behaviour of a CHG device. In particular, we shall focus on the case of the project FERMI@Elettra [7] and assume the experimental setting relative to the output wavelength 100 nm. In this case, $n = 3$ (i.e., the initial seed wavelength is 100 nm), $\gamma = 2348$, $\sigma_\gamma = 150$ KeV and $\rho = 3 \cdot 10^{-3}$. Direct numerical simulations are performed using GENESIS [8], a three dimensional code that explicitly accounts for the coupling between the transverse and longitudinal dimensions. Assuming a radiator length of 16 m, a horizontal and vertical (normalized) beam emittance of $1.5 \mu\text{m}$ and on optical waist of $w \simeq 300 \mu\text{m}$, simulations give an output power of about 3 GW.

Independently, one can calculate the value of $|b_0|$ and p_0 by inserting the nominal values of the relevant parameters in equations 18-16. Then, Lynden-Bell theory enables us to predict the QSS value for the intensity which are shown to correlate extremely well with Genesis based calculation, the disagreement being quantified in at most 10 % [9].

CONCLUSIONS

The theoretical approach outlined in this paper constitutes a novel strategy to predict the intensity at saturation

for a CHG setting, provided the value of the incoherent energy spread is assigned and without involving to direct numerical investigations.

The short recipe goes as follows: by knowing σ_γ one can calculate $\sigma_{\gamma,tot}$ by means of eq.(17) and consequently estimate both $|b_0|$ and p_0 , based on eqs.(16)–(18). The spatial width, θ_0 , of the initial water-bag distribution (here assumed to mimic the more natural Gaussian profile) is eventually obtained upon inversion of relation $|b_0| = \sin(\theta_0)/\theta_0$. Once the values of θ_0 and p_0 are given, the theory of the violent relaxation allows to quantitatively predict the saturated state of the system.

Finally let us stress that the applicability of the method we have developed is currently limited to situations in which transverse effects are neglected. This in turn entails the possibility of assuming the electron-beam geometrical emittance smaller than the radiation wavelength, the beam relative energy spread smaller than ρ and the Rayleigh length of emitted radiation much longer than the radiator length. These conditions apply for instance to the case of the whole spectral range that is to be covered by the FERMI@Elettra FEL (100-10 nm).

REFERENCES

- [1] L. H. Yu, *Phys. Rev. A* **44** 5178 (1991).
- [2] T. Dauxois, S. Ruffo, E. Arimondo, M. Wilkens (Eds), *Lecture Notes in Physics 602, Springer Dynamics and Thermodynamics of Systems with Long Range Interactions* (2002).
- [3] A. Antoniazzi, D. Fanelli, J. Barré, P. H. Chavanis, T. Dauxois, S. Ruffo, submitted to *Phys. Rev. Lett.* (2006).
- [4] J. Barré *et al.*, *Phys. Rev. E* **69** 045501 (2004).
- [5] D. Lynden-Bell, *Mon. Not. R. Astron. Soc.* **136**, 101 (1967).
- [6] P. H. Chavanis, J. Sommeria, R. Robert, *Astrophys. J.* **471**, 385 (1996).
- [7] See <http://www.elettra.trieste.it/FERMI/>.
- [8] <http://pbpl.physics.ucla.edu/reiche/>.
- [9] F. Curbis, A. Antoniazzi, G. De Ninno, D. Fanelli, preprint submitted to *Phys. Rev. E* (2006).

¹Note that in deriving equation (16) an optimization scheme for the bunching parameter has been put forward according to the standard experimental procedure. A detailed account on the approximations involved is presented in [9] starting from the usual expression given in [1]